IJST (2015) 39A4: 551-558
Iranian Journal of Science & Technology

http://ijsts.shirazu.ac.ir

Analysis of couple stress fluid in helical screw rheometer

M. A. Javed[1]*, N. Ali[1] and M. Sajid[2]

[1]*Department of Mathematics & Statistics, FBAS, International Islamic University Islamabad 44000, Pakistan*
[2]*Theoretical Physics Division, PINSTECH, P.O. Nilore, Islamabad 44000, Pakistan*
E-mail: rana_asif_iiui@yahoo.com

Abstract

In this paper, the flow of couple stress fluid is investigated in a helical screw rheometer (HSR). By unwrapping the channel, lands, and the outside rotating barrel, the geometry of HSR is approximated as a shallow infinite channel. Both one- and two-dimensional analysis of the problem is presented using rectangular coordinates. In either case an exact solution of the flow problem is presented and the formulas of velocity profile and volumetric flow rate are obtained as a function of couple stress parameter. It is observed that velocity profile decreases in going from Newtonian to couple stress fluid which indicates a decrease in extrusion process for a couple stress fluid in comparison with Newtonian fluid. Moreover, the volumetric flow rate is found to be a decreasing function of couple stress parameter.

Keywords: Couple stress fluid; helical screw rheometer (hsr); volumetric flow rate; exact solution

1. Introduction

Foodstuffs in many instances are concentrated suspensions that exhibit a very complex rheological behavior. Examples includes chocolate, fruit juices, ketchup, wheat flour dough and dairy products such as yogurts. The understanding and measurements of rheological properties of the foodstuffs during food processes are necessary to obtain the desired quality and shape of the product. Several types of viscometers have been used to measure rheological properties of food. Among these, rotational viscometers are most common. These include: concentric cylinder viscometer, cone and plate viscometer, parallel plate viscometer. Apart from these viscometers tube and slit viscometers are also used by food engineers to determine the rheological properties of various extruded food material (Steffe, 1996). Mixer viscometer is another type of viscometers which has been successfully used by various researchers to measure rheological behavior of reacting biological material, fresh concrete and to chemorheological studies involving starch gelantinization (Tattersall, 1983, Dolan, 1990). Helical screw rheometer (HSR) is a type of mixer viscometer which was proposed by (Kraynik et al., 1984) and successfully used for tomato product (Tamura, 1989a). The instrument consists of a helical screw in a tight fitted barrel and resembles a single screw extruder with a close discharge. Particle suspension is maintained by screw rotation and rheological properties are correlated to pressure drop over the length of the screw. Initial theoretical study pertaining to flow in HSR was performed by Tamura et al. (1993b). They presented theoretical one- and two-dimensional analysis for Newtonian fluid using rectangular and cylindrical coordinates. For non-Newtonian power law model they presented a one- dimensional rectangular analysis. Their work was followed in some recent attempts by Siddiqui et al., (2013, Zeb et al., 2014). In one paper (Siddiqui et al., 2013), the author's analyzed flow of a third grade fluid in HSR using Adomian decomposition technique while in Zeb et al., (2014) the flow analysis in HSR is developed for an Eyring-Powell fluid. As stated in the beginning of the introduction, concentrated suspensions are widely encountered in food industry. Since suspensions are basically a mixture of fluid and solid particles, a theoretical analysis which might shed light on extrusion of such suspensions should take into account particle size effects. One such model which takes into account particle size effect is couple stress fluid model. In the category of non-Newtonian fluids, couple stress fluid has distinct features such as polar effects in addition to possessing large viscosity. The theory of couple stress was developed by (Stokes, 1966). This theory generalizes the classical Navior-Stokes theory to allow for polar effects such as presence of couple stresses and body couples. The main effects of couple stresses are introduction of size dependent effects that are not present in the classical viscous theory. In classical viscous theory the stress tensor

*Corresponding author
Received: 10 August 2014 / Accepted: 27 January 2015

is symmetric, which is the result of the assumption that there is no rotational interaction among particles. However, this is not true for the cases of fluid flow with suspended particles and thus need for couple stress theory arises. In fact, the micro rotation of suspended particles gives rise to an anti-symmetric stress, known as couple stress. Couple stress theory is found quite useful in description of various types of lubricants, blood, suspension fluids, etc. (Srinivasacharya and Kaladher, 2011). Some studies regarding couple stress fluid in different scenarios can be found in refs. (Srivastava., 1986, El-Shehawey et al., 1994, Ali et al., 2007, Pal et al. 1988, Naduvinamani et al., 2005, Srinivasacharya et al, 2009, Lin et al, 2007, Hayat et al., 2013, Tadmor et al., 1970).

Motivated by the above facts, we, in this paper, put forward a theoretical flow analysis of couple stress fluid in helical screw rheometer. The paper is organized in the following manner. Constitutive equation of couple stress fluid is presented in section 2. One dimensional flow analysis is performed in section 3. Section 4 presents a theoretical two-dimensional analysis. The obtained results are explained in section 5. We conclude the paper in section 6.

2. Basic Equations

For a couple stress fluid the constitutive equations and equation of motion in the absence of body force and body couple are (Stokes, 1966):

$$T_{ji,j} = \rho \frac{dv_i}{dt}, \tag{1}$$

$$e_{ijk} T^A_{jk} + M_{ji,j} = 0, \tag{2}$$

$$\tau_{ij} = -p\delta_{ij} + 2\mu d_{ij}, \tag{3}$$

$$\mu_{ij} = 4\eta w_{j,i} + \eta' w_{i,j}, \tag{4}$$

where v_i is the velocity vector, τ_{ij} and T^A_{ij} are the symmetric and anti-symmetric parts of the stress tensor T_{ij} respectively, M_{ij} is the couple stress tensor, μ_{ij} is the deviatoric part of M_{ij}, w_i is the vorticity vector, d_{ij} is the symmetric part of the velocity gradient, η and η' are the constants associated with the couple stress, p is the pressure, and the other terms have their usual meaning from tensor analysis.

3. One-dimensional rectilinear flow analysis

Let us consider flow of an incompressible couple stress fluid in a helical screw rheometer. The helical channel is unwrapped ignoring the effects of curvature. As suggested by (Tadmor and Klein, 1970) and later cited by (Tamura et al. 1993), it is easy to visualize is the "unwrapping" of screw by rotating the screw, with ink-painted flights, on a piece of paper. The trace left on the paper would be the "unwrapped" channel. Thus complicated geometry of helical screw rheometer is approximated as a shallow infinite rectangular channel by assuming $L/h << 1$; where *L* and *h* are the width and depth of the channel, respectively. The lower plate which is screw surface is stationary and the upper plate, the barrel surface, moves across the top of the channel with velocity V_0 at an angle ϕ to the direction of the channel. The phenomenon remains unaltered if it is assumed that the barrel is stationary and the screw is rotating. The rectangular coordinate are positioned in such a way that *x* is the axial direction and *z* coincides with the direction of the screw rotation. The flow is assumed to occur in the *xz*-plane only, hence the velocity profile is

$$V = [0, 0, w(y)]. \tag{5}$$

In such case the dominant flow is in the *z*-direction except for circulation near the flights, which is considered negligible for a narrow gap relative to the width of the channel. The fluid then flows only in the direction of the barrel rotation from *A* to *A′* as shown in Fig. 1. The flow analysis initially focuses across this cross-channel, rather than the total unwrapped helical channel. As determined above there is only one velocity component, *w = w(y)*. So the momentum equation (1) in the absence of gravity reduce to

$$0 = -\frac{\partial p}{\partial z} + \mu \frac{d^2 w}{dy^2} - \eta \frac{d^4 w}{dy^4}, \tag{6}$$

with the boundary conditions

$$w = 0, \ , \ \frac{d^2 w}{dy^2} = 0 \qquad \text{at } y = 0, \tag{7}$$

$$w = V_0, \ \frac{d^2 w}{dy^2} = 0 \qquad \text{at } y = h \tag{8}$$

The second boundary conditions in (7) and (8) results from the assumption of removing of couple stresses near the walls. Eq. (6) can be easily solved subject to boundary conditions (7) and (8) to get

$$w(y)=\left(\frac{V_0}{h}-\frac{h}{2\mu}\frac{dp}{dz}\right)y+\frac{1}{2\mu}\frac{dp}{dz}y^2+$$
$$\frac{\eta}{\mu^2}\frac{dp}{dz}+\frac{\eta}{2\mu^2}\frac{dp}{dz}\frac{\left(e^{-\gamma}-1\right)e^{\sqrt{\frac{\mu}{\eta}}y}}{\sinh\gamma}+ \quad (9)$$
$$\frac{\eta}{2\mu^2}\frac{dp}{dz}\frac{\left(1-e^{\gamma}\right)e^{-\sqrt{\frac{\mu}{\eta}}y}}{\sinh\gamma}.$$

In order to make expression (9) dimensionless, we introduce

$$w^*=\frac{w}{V_0}, y^*=\frac{y}{h} \quad (10)$$

and get

$$w(y)=y+\frac{h^2}{\mu V_0}\frac{dp}{dz}\left[\frac{y^2-y}{2}+\frac{1}{\gamma^2}\right.$$
$$\left.+\frac{\sinh\left(y-1\right)\gamma-\sinh y\gamma}{2\gamma^2\sinh\gamma}\right], \quad (11)$$

where $*$ is dropped for simplicity.

The first term on the right side of Eq. (11) is to be drag velocity and the second term is the pressure flow velocity. The drag flow velocity is linear, whereas the pressure flow velocity is parabolic due to pressure gradient caused by the presence of the screw flights. The flow rate per unit width, obtained by integrating the velocity across the gap is

$$\frac{Q}{hV_0}=\int_0^1 w dy. \quad (12)$$

Substitution of (11) into (12) yields

$$Q=\frac{hV_0}{2}+\frac{h^3}{12\mu}\left(-\frac{dp}{dz}\right)\left[1-\frac{12}{\gamma^2}+\frac{12}{\gamma^3}\tanh\gamma\right]. \quad (13)$$

The first term on right side of the above equation is drag flow rate, whereas the second term is pressure flow rate. When the screw is rotated, instead of the barrel the entire channel moves while the plate remains stationary. Thus to the stationary observer, there is an apparent net flow per unit width of $Q = V_0h$. Thus we can write from Eq. (13)

$$0=-\frac{hV_0}{2}+\frac{h^3}{12\mu}\left(-\frac{dp}{dz}\right)\left[1-\frac{12}{\gamma^2}+\frac{12}{\gamma^3}\tanh\gamma\right]. \quad (14)$$

Rearranging, we get

$$\frac{\Delta p}{\Delta z}=-\frac{6\mu V_0\left(\sqrt{\frac{\mu}{\eta}}h\right)^3}{h^2\left(\left(\sqrt{\frac{\mu}{\eta}}h\right)^3-12\left(\sqrt{\frac{\mu}{\eta}}h\right)+12\tanh\sqrt{\frac{\mu}{\eta}}h\right)}, \quad (15)$$

where Δp is pressure difference within the channel and Δz corresponds to channel width, πD. Moreover $V_0=\pi DN$ where *N* is the rate of rotation. Thus Eq. (15) becomes

$$\mu=-\frac{\Delta p}{6\pi^2D^2N}$$
$$\frac{h^2\left(\left(\sqrt{\frac{\mu}{\eta}}h\right)^3-12\left(\sqrt{\frac{\mu}{\eta}}h\right)+12\tanh\sqrt{\frac{\mu}{\eta}}h\right)}{\left(\sqrt{\frac{\mu}{\eta}}h\right)^3}. \quad (16)$$

This equation can be used to calculate the material parameter η of couple stress fluid for given values of μ, h, V_0 and *dp/dz*. The presence of constant pressure gradient maintained in the HSR is responsible for the effects of couple stresses. If *dp/dz =0* the effects of couple stress are negligible and therefore in that case the value of μ can be determined experimentally. This value of μ can be used in formula (15) to obtained a value of η.

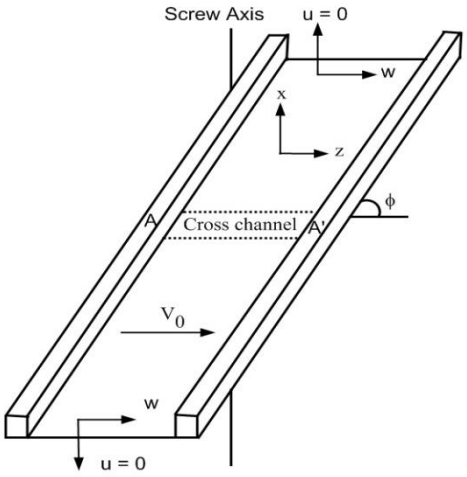

Fig. 1. Helical channel approximated as a rectangular channel

4. Mathematical formulation for two-dimensional flow analysis

The two-dimensional flow analysis differs from the previous one-dimensional analysis in the positioning of the coordinate axes. Here the rectangular coordinates are positioned in such a way that *x*-axis is perpendicular to the channel wall or flights and *z*-axis coincide with the down channel direction. The flow has two velocity components, a cross channel component, *u*, and a down channel component, *w*. For simplicity, the velocity of the barrel relative to the channel (V_0) is resolved into two components *U* and *W* which are along *x*- and *z* -axes, respectively. The geometry of the problem is explained in Fig. 2.

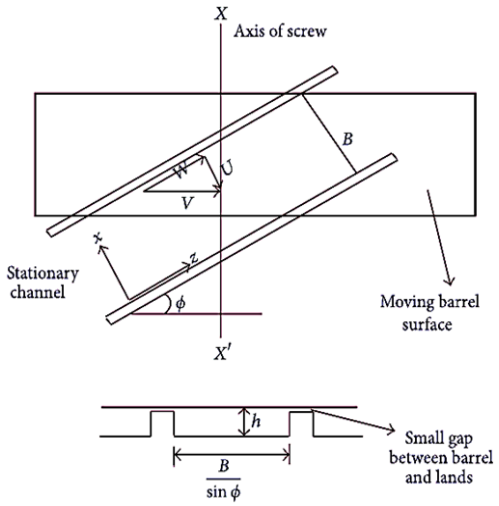

Fig. 2. The geometry of the unwrapped screw channel and barrel surface

The geometry of the problem suggests that the velocity field is

$$V=[u(y),0,w(y)]. \tag{17}$$

In view of (17), Eq. (1) can be written in component form as

$$0=-\frac{\partial p}{\partial x}+\mu\frac{d^2u}{dy^2}-\eta\frac{d^4u}{dy^4}, \tag{18}$$

$$0=-\frac{\partial p}{\partial y}, \tag{19}$$

$$0=-\frac{\partial p}{\partial z}+\mu\frac{d^2w}{dy^2}-\eta\frac{d^4w}{dy^4}, \tag{20}$$

The associated boundary conditions are

$$u=0,\quad w=0,\frac{d^2u}{dy^2}=0,\quad \frac{d^2w}{dy^2}=0\quad \text{at}\quad y=0, \tag{21}$$

$$u=U,\quad w=W,\quad \frac{d^2u}{dy^2}=0,\quad \frac{d^2w}{dy^2}=0\quad \text{at}\quad y=h, \tag{22}$$

Where

$$U=-V_0Sin\phi,\qquad W=V_0Cos\phi.$$

It is again mentioned here that the boundary conditions $d^2u/dy^2=0,\ d^2w/dy^2=0$ at *y=0* and *y=h* results from the assumption of removing couple stresses at the walls.

Introducing the non dimensionlized parameters

$$x^*=\frac{x}{h},\ y^*=\frac{y}{h},\ z^*=\frac{z}{h},\ u^*=\frac{u}{W},$$
$$w^*=\frac{w}{W},\ p^*=\frac{p}{\mu(W/h)},\ \gamma^2=\frac{\mu h^2}{\eta}, \tag{23}$$

Eqs. $(18)-(22)$ after dropping the asterisk can be cast as

$$0=-\frac{\partial p}{\partial x}+\frac{d^2u}{dy^2}-\frac{1}{\gamma^2}\frac{d^4u}{dy^4}, \tag{24}$$

$$0=-\frac{\partial p}{\partial x}+\frac{d^2u}{dy^2}-\frac{1}{\gamma^2}\frac{d^4u}{dy^4}, \tag{25}$$

$$u=0,\quad w=0,\quad \frac{d^2u}{dy^2}=0,\quad \frac{d^2w}{dy^2}=0\ \text{at}\quad y=0, \tag{26}$$

$$u=\frac{U}{W},\quad w=1,\quad \frac{d^2u}{dy^2}=0,\quad \frac{d^2w}{dy^2}=0\quad \text{at}\quad y=1, \tag{27}$$

4.1. Solution of the Problem

A solution of Eqs. (24) and (25) subject to boundary conditions (26) and (27) turns out to be

$$u=\frac{1}{\gamma^2}\frac{\partial p}{\partial x}+\frac{U}{W}y+\left(\frac{y^2-y}{2}\right)\frac{\partial p}{\partial x}+\left[\frac{\mathrm{Sinh}(y\gamma-\gamma)-\mathrm{Sinh}\gamma y}{\gamma^2\,\mathrm{Sinh}\gamma}\right]\frac{\partial p}{\partial x}, \tag{28}$$

$$w=\frac{1}{\gamma^2}\frac{\partial p}{\partial z}+y+\left(\frac{y^2-y}{2}\right)\frac{\partial p}{\partial z}+\left[\frac{\mathrm{Si}nh(y\gamma-\gamma)-\mathrm{Si}nh\gamma y}{\gamma^2\,\mathrm{Si}nh\gamma}\right]\frac{\partial p}{\partial z}, \tag{29}$$

4.2. Velocity in the direction of the axis of screw

The velocity in the direction of the axis of the screw at any depth in the channel can be computed from (28) and (29) as

$$s=w\sin\phi+u\cos\phi, \tag{30}$$

$$s=\left\{\frac{1}{\gamma^2}\frac{\partial p}{\partial z}+y+\left(\frac{y^2-y}{2}\right)\frac{\partial p}{\partial z}+\left[\frac{\mathrm{Si}nh(y\gamma-\gamma)-\mathrm{Si}nh\gamma y}{\gamma^2\,\mathrm{Si}nh\gamma}\right]\frac{\partial p}{\partial z}\right\}\sin\phi+\left\{\frac{1}{\gamma^2}\frac{\partial p}{\partial x}+\frac{U}{W}y+\left(\frac{y^2-y}{2}\right)\frac{\partial p}{\partial x}+\left[\frac{\mathrm{Si}nh(y\gamma-\gamma)-\mathrm{Si}nh\gamma y}{\gamma^2\,\mathrm{Si}nh\gamma}\right]\frac{\partial p}{\partial x}\right\}\cos\phi. \tag{31}$$

which show the resultant velocity of the flow.

4.3. Volumetric flow rates

Volumetric flow rate in *x*-direction per unit width is

$$Q_x^*=\int_0^1 u\,dy, \tag{32}$$

where $Q_x^*=Q/WhL$ is dimensionless volumetric flow rate in the x-direction. Using equation (28) in the above equation gives

$$Q_x^*=\frac{U}{2W}+\left(\frac{1}{\gamma^2}-\frac{1}{12}\right)\frac{\partial p}{\partial x}-2\frac{\tan\frac{\gamma}{2}}{\gamma^3}\frac{\partial p}{\partial x}, \tag{33}$$

Similarly, volumetric flow rate in z-direction per unit width is

$$Q_z^*=\int_0^1 w\,dy, \tag{34}$$

where $Q_z^*=Q/WhL$ is dimensionless volumetric flow rate in the z-direction. Using equation (29) in the above equation gives

$$Q_z^*=\frac{1}{2}+\left(\frac{1}{\gamma^2}-\frac{1}{12}\right)\frac{\partial p}{\partial z}-2\frac{\tan\frac{\gamma}{2}}{\gamma^3}\frac{\partial p}{\partial z}. \tag{35}$$

The resultant volumetric flow rate forward in the screw channel, which is the product of the resultant velocity and cross-sectional area integrated from the root of the screw to the barrel surface is

$$Q^*=\frac{n}{\sin\phi}\int_0^1 s\,dy, \tag{36}$$

where $Q^*=Q/WhL$ dimensionless volumetric is flow rate in the direction of the screw and n is the number of parallel flights in a multiflight screw. From Eq. (31) and (36), we get

$$Q^*=\frac{n}{12W\gamma^2\sin\phi}\left[\left(6U\gamma^3-\frac{\partial p}{\partial x}W\gamma(-12+\gamma^2)\right)\cos\phi+W\gamma\left(6\gamma^2-\frac{\partial p}{\partial z}(-12+\gamma^2)\right)\sin\phi-24W\left(\frac{\partial p}{\partial x}\cos\phi+\frac{\partial p}{\partial z}\sin\phi\right)\tan\frac{\gamma}{2}\right] \tag{37}$$

5. Results and discussion

In this section, the solution obtained for the steady flow of an incompressible and homogenous couple stress fluid in helical screw rheometer (HSR) is analyzed for various emerging parameters. Here we discussed the effect of dimensionless couple stress parameter $\acute{\epsilon}$ and pressure gradients $\partial p/\partial x$ and $\partial p/\partial z$, on the velocity profile with the help of graphical representations. From Figs. 3–5, we can observe that the velocity profiles *u(y)*, *w(y)* and *s(y)* show an increasing trend with an increase in the value of couple stress parameter γ. It is also observed that both *u* and *w* component of velocity show linear behavior for small values of γ. Moreover, the maximum in *u* component of velocity occurs near the screw while it occurs near the barrel for *w* component of velocity. Figure 6 shows that the resultant velocity *s* is parabolic and and increases by increasing γ thereby indicating a decrease in the extrusion process for small value of γ. From Figs. 7 and 8, we observe that an increase in pressure gradient (either of $\partial p/\partial x$ or $\partial p/\partial z$) causes an increase in the magnitude of velocity profiles *u(y)* and *w(y)*. Further, an increase in pressure gradient $\partial p/\partial x$ pushes the fluid toward

screw while for higher values of $\partial p/\partial z$, the fluid is pushed toward the barrel. Figure 9 depicts that resultant velocity increases by increasing the value of pressure gradient. The effects of $\partial p/\partial x$ and $\partial p/\partial z$ on resultant volume flow rate *Q* are shown in Figs. 10 and 11. It is interesting to note that volumetric flow rate *Q* increases by increasing pressure gradient. However, it decreases by increasing the couple stress parameter γ and asymptotically approaches to a constant Newtonian value. Figure 12 depicts the effects of flight angle ϕ on *s*. This figure shows that resultant velocity *s* increases by increasing the flight angle ϕ.

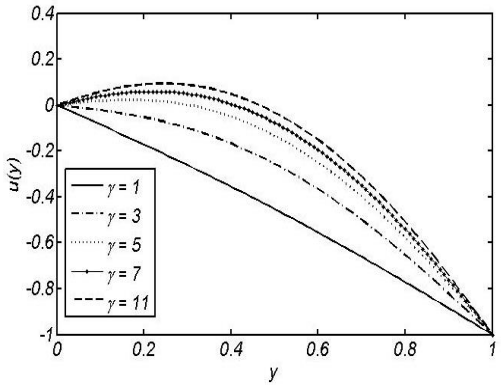

Fig. 3. Velocity profile $u(y)$ for various values of γ with $\partial p/\partial x = -4$ and $\phi = 45^\circ$

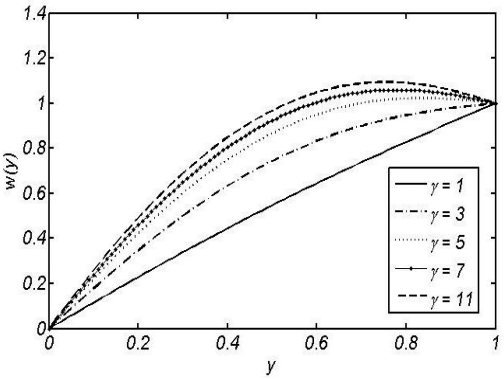

Fig. 4. Velocity profile $w(y)$ for various values of γ with $\partial p/\partial z = -4$ and $\phi = 45^\circ$

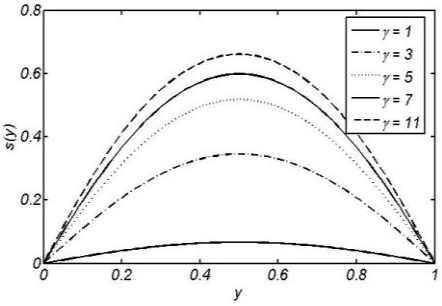

Fig. 5. Velocity profile $s(y)$ for various values of γ with $\partial p/\partial x = \partial p/\partial z = -4$ and $\phi = 45^\circ$

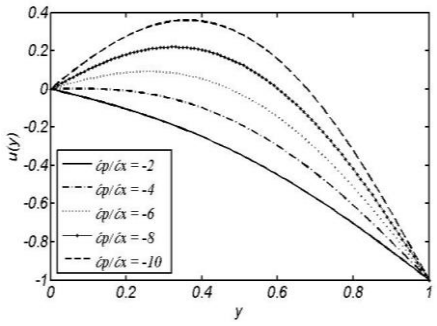

Fig. 6. Velocity profile $u(y)$ for different values of $\partial p/\partial x$ with $\gamma = 4, \partial p/\partial z = -4$ and $\phi = 45^\circ$

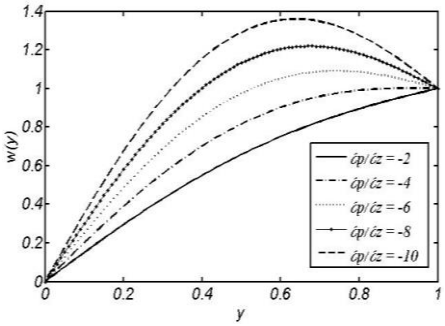

Fig. 7. Velocity profile $u(y)$ for different values of $\partial p/\partial z$ with $\gamma = 4, \partial p/\partial x = -4$ and $\phi = 45^\circ$

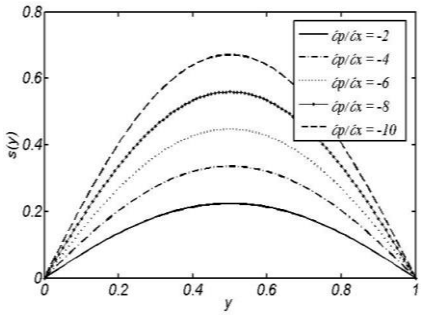

Fig. 8. Velocity profile $s(y)$ for different values of $\partial p/\partial x$ with $\gamma = 4, \partial p/\partial z = -4$ and $\phi = 45^\circ$

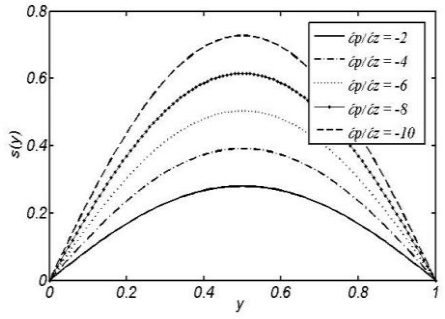

Fig. 9. Velocity profile $s(y)$ for different values of $\partial p/\partial z$ with $\gamma = 4 \partial p/\partial x = -4$ and $\phi = 45^{\circ}$

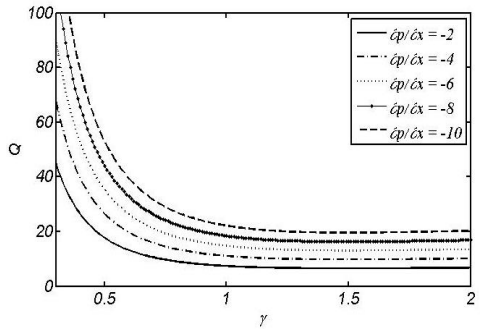

Fig. 10. Volumetric flow Q for different values of $\partial p/\partial x$ with $\gamma = 4, \partial p/\partial z = -2, n = 1$ and $\phi = 45^{\circ}$

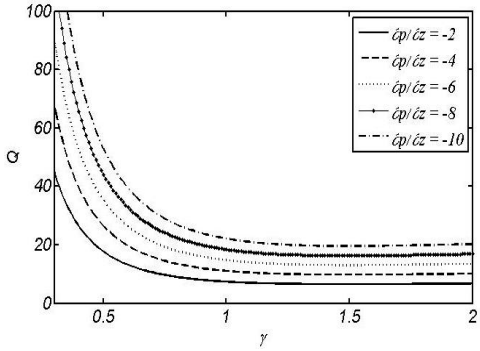

Fig. 11. Volumetric flow Q for different values of $\partial p/\partial z$ with $\gamma = 4, \partial p/\partial x = -2, n = 1$ and $\phi = 45^{\circ}$

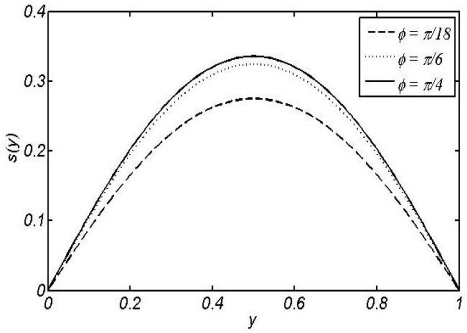

Fig. 12. Velocity profile $s(y)$ for different values of ϕ with $\gamma = 4,$ and $\partial p/\partial x = \partial p/\partial z = -4.$

6. Concluding remarks

The steady flow of the incompressible, homogenous couple stress fluid is investigated in helical screw rheometer (HSR). By performing a one-dimensional flow analysis a transcendental equation is presented for calculating the value couple stress parameter experimentally. For two-dimensional problem the exact expression of velocity profiles, flow rate and average velocity of the problem are calculated. We observed that the velocity field depends strongly on the involved parameter and pressure gradient. By increasing the value of non-dimensional parameter γ the resultant velocity increases. It is also noted that flow rate decreasing by increases the values of γ. The present analysis is performed with the hope that it might shed some light on extrusion of fluid food suspensions.

Acknowledgements

The first author is grateful to the Higher Education Commission of Pakistan for financial assistance.

References

Ali, N., Hayat, T., & Sajid, M. (2007). Peristaltic flow of a couple-stress fluid in an asymmetric channel. *Biorheology*, 44, 125–138.

Dolan, K. D., & Steffe, J. F. (1990). Modeling the rheological behavior of gelatinizing starch solutions using mixer viscometry data. *Journal of Texture Studies*, 21, 265–294.

El-Shehawey, E. F., & Mekheimer, K. S. (1994). Couple-stresses in Peristaltic transport of fluid. *Journal of Physics D*, 27, 1163–1170.

Hayat, T., Iqbal, Z., & Alsaedi, A. (2013). Stagnation-point flow of couple stress fluid with melting heat transfer. *Journal of Applied Mathematics & Mechanics*, 34(2), 167–176.

Kraynik, A. M., Aubert, J. H., & Chapman, R. N. (1984). Helical screw rheometer: A new concept in rotational rheometry. *Sandia National Laboratories, Albuquerque, NM, USA.*

Lin, J. R., & Hung, C. R. (2007). Combined effects of non-Newtonian couple stresses and fluid inertia on the squeeze film characteristics between a long cylinder and an infinite plate. *Fluid Dynamics. Research*. 39, 616–631.

Naduvinamani, N. B., Hiremath, P. S., & Gurubasavaraj, G. (2005). Effects of surface roughness on the couple stress squeeze film between a sphere and a flat Plate. *Tribology International*, 38, 451–458.

Pal, D., Rudraiah, N., & Devananthan, R. (1988). A couple stress model of blood flow in the

microcirculation. *Bulletin of Mathematical Biology*, 50, 329–344.

Srinivasacharya, D., & Kaladher, K. (2011). Mixed convection in a couple stress fluid with Soret and Dufour effects. *International Journal of Applied Mathematics & Mechanics*, **7**, 59–71.

Srinivasacharya, D., Srinivasacharyulu, N., & Odelu, O. (2009). Flow and heat transfer of couple stress fluid in a porous channel with expanding and contracting walls. Int. Commun. Heat Mass, 36, 180–185.

Srivastava, L. M. (1986). Peristaltic transport of a couple-stress fluid. *Rheologica Acta*, 25, 638–641.

Steffe, J. F. (1996). Rheological methods in food process engineering. *Second Edition, Freeman Press.*

Stokes, V. K. (1966). Couple stress fluid. *Physics Fluids*, 9, 1709–1715.

Tadmor, Z. & Klein, I. (1970). Engineering principles of plasticating extrusion. Van Nostrand Reinhold Co., New York.

Tamura, M. S., Henderson, J. M., Powell, R. L., & Shoemaker, C. F. (1989). Evaluation of the helical screw rheometer as an on-line viscometer. *Journal of Food Sciences*. 54, 483–484.

Tamura, M. S., Henderson, J. M., Powell, R. L. & Shoemaker, C. F., (1993). Analysis of the helical screw rheometer for fluid food. *Journal of Food Process Engineering*, 16(2), 93–126.

Tattersall, G. H., & Banfill, P. F. G. (1983). The rheology of fresh concrete. *Pitman Publishing Inc. Boston.*

Zeb, M., Islam, S., Siddiqui, A. M., & Haroon, T. (2013). Analysis of third-grade fluid in helical screw rheometer. *Journal of Applied Mathematics*, 2013, pp.11.

Zeb, M., Islam, S., Siddiqui, A. M., & Haroon, T. (2014). Analysis of Eyring-Powell fluid in helical screw rheometer. *Journal of Applied Mathematics*, 2014, pp. 14.